ISSN 0006-2979, Biochemistry (Moscow), 2010, Vol. 75, No. 2, pp. 201-207. © Pleiades Publishing, Ltd., 2010.
Published in Russian in Biokhimiya, 2010, Vol. 75, No. 2, pp. 247-255.
Originally published in Biochemistry (Moscow) On-Line Papers in Press, as Manuscript BM09-197, January 17, 2010.

Selenoprotein W Depletion *in vitro* Might Indicate that Its Main Function Is Not as an Antioxidative Enzyme

Wang Xiao-Long[1,2], Yang Chuan-Ping[2]*, Xu Kai[1], and Qin Ou-Jv[1]

[1]*Biomedicine Division, Wildlife Resource College, Northeast Forestry University, Ministry of Education, P. R. China*
[2]*Key Laboratory of Forest Tree Genetics Improvement and Biotechnology, Ministry of Education, P. R. China; E-mail: ch_p.yang@yahoo.com.cn*

Received July 3, 2009
Revision received September 13, 2009

Abstract—Examination of the antioxidative homeostasis in skeletal muscle cells in the presence or absence of selenoprotein W (SelW) is necessary to understand the importance of SelW in the antioxidative system. Depletion of SelW by RNA interference was achieved by introducing a synthetic small interfering RNA into the mouse skeletal muscle cell line C2C12 (C3H). Transfectant screening was performed by real-time reverse transcription-PCR, Western blotting, flow cytometry, fluorescence staining, cell viability, and glutathione assays. SelW expression and mRNA levels were downregulated by 62.1 and 72.4%, respectively. In addition, acute cytotoxicity and an apoptosis rate of ~36% in SelW-depleted cells demonstrated that RNA interference was successful. As compared with non-SelW-depleted cells, the enzyme activities of glutathione peroxidase, superoxide dismutase, and catalase and total antioxidative capability and glutathione level increased by 47.6, 103.0, 31.0, 205.6, and 30.0%, respectively ($P < 0.05$). Thus, SelW is important for the antioxidative system of muscle cells. Depletion of SelW, however, could be compensated by other intracellular antioxidative enzymes because oxidative stress was not the causative factor for apoptosis in SelW-depleted cells. Thus, the main function of SelW in muscle cells is not in the antioxidative system.

DOI: 10.1134/S0006297910020100

Key words: selenoprotein W, function, RNA interference, antioxidation, muscle cell, *in vitro*

The antioxidative function of selenoproteins plays a very important role in the pathophysiological course of many diseases, and selenoprotein deficiencies can result in oxidative damage to cells and the body [1]. The function of selenoprotein W (SelW), which was first purified more than 10 years ago [2], remains to be determined. Bioinformatics and current empirical studies suggest that SelW mainly functions in an antioxidative capacity. Only a few reports have examined the calmodulin-like motif of SelW, and the function of its gene structure remains unknown [3].

Abbreviations: CAT, catalase; FITC, fluorescein isothiocyanate; GPx, glutathione peroxidase; GSH, glutathione; MTT, 3-(4,5-dimethylthiazol-2-yl)-2,5-diphenyltetrazolium bromide; PI, propidium iodide; SelW, selenoprotein W; siRNA, small interfering RNA; SOD, superoxide dismutases; T-AOC, total antioxidative capability; WST-1, 2-(4-iodophenyl)-3-(4-nitrophenyl)-5-(2,4-disulfophenyl)-2H-tetrazolium, monosodium salt.

* To whom correspondence should be addressed.

SelW is the selenoprotein that is specifically involved in striated muscle tropism [4]; its activity and expression correlate positively with selenium intake. SelW is difficult to detect in muscle tissue of selenium-deficient animals [5, 6], and SelW expression in cells is sensitive to Se-depletion [7]. Thus, researchers hypothesize that SelW depletion causes Keshan disease in humans and white muscle disease in animals [8, 9]. In 1996, Beilstein et al. [10] determined that a cysteine residue in SelW forms a covalent bond with glutathione (GSH) and that SelW noncovalently binds certain 44-Da moieties. The sequence of SelW (as deduced from the mRNA) indicated that SelW is a typical selenoprotein that contains a selenocysteine insertion sequence [11], and the gene sequences of five mammalian SelW homologs are 80% identical [12]. Moreover, SelW proteins from different mammals exhibit 83% amino acid sequence identity [5]. In 2002, Jeong et al. [13] verified that SelW is a GSH-dependent antioxidant *in vivo*. A later report revealed that SelW has a broad expression pattern and that aerobic growth conditions produce a mutant form of SelW with-

out bound GSH, whereas anaerobic conditions produce a GSH-bound form [14]. In proliferating myoblasts, SelW exhibits an immediate response to oxidative stress after exposure to hydrogen peroxide [15]. SelW belongs to a family of reduction/oxidation (redox) enzymes and contains a redox motif [16, 17], and thus it is hypothesized to function in antioxidation. However, overexpression or underexpression of SelW in rat glial cells under different conditions suggests that SelW does not function in an antioxidative capacity [18]. Thus, the role of SelW in antioxidation remains unclear.

We hypothesized that if SelW mainly serves as an antioxidant in muscle cells, then its depletion may result in changes in the antioxidative system, yielding irreversible damage to muscle tissue. Hence, we examined changes in the antioxidative capacity of muscle cells as well as changes in the levels of important antioxidative enzymes upon depletion of SelW by RNA interference. SelW knockdown significantly increased the activities of antioxidative enzymes (and glutathione level), resulting in cytotoxicity and apoptosis of muscle cells. These results suggest that muscle cell apoptosis is not caused by oxidative stress, which further supports the idea that SelW does not play a crucial role in the antioxidative system.

MATERIALS AND METHODS

Cell culture. The C2C12 (C3H) mouse myoblast cell line derived from skeletal muscle was obtained from the Cell Center of the Chinese Academy of Medical Sciences (Beijing) and cultured in Dulbecco's modified Eagle's medium (DMEM) with 4 mM L-glutamine (HyClone, USA) and supplemented with 10% (v/v) fetal bovine serum (HyClone) at 37°C with 5% CO_2 in a humidified chamber (Shallab, USA) following the instructions of the American Type Culture Collection. Antibiotics were not used during culturing to avoid cytotoxicity.

Design and synthesis of small interfering RNAs (siRNAs). Online siRNA design software (www.genscript.com) was used to design and select three pairs of 21-bp siRNAs (one positive acting, one negative control, and one fluorescently labeled reporter) according to the *Mus musculus* SelW gene sequence (Accession: BC052719). The pairs of siRNA were produced by Shanghai GenePharma Co. (P. R. China): positive-acting pair, 5′CGCCGUUCGAGUCGUGUAUTT3′, 5′AUACACGACUCGAACGGCGAG3′; negative control pair, 5′UUCUCCGAACGUGUCACGUTT3′, 5′ACGUGACACGUUCGGAGAATT3′; fluorescently labeled pair, 5′UUCUCCGAACGUGUCACGUTT3′, 5′ACGUGACACGUUCGGAGAATT3′.

RNA interference. *Transfection.* The day before transfection, cells were trypsinized (0.1% trypsin/0.02% EDTA) and plated at a density of $5 \cdot 10^5$ cells/ml to achieve 50-80% confluency the following day. Three groups were analyzed: positive group (pair 1 siRNA), negative control group (negative control siRNA), and a blank group (no siRNA). For transfection, 1 μg siRNA/well was chosen according to a pilot experiment and the manufacturer's instructions for Lipofectamine and Plus reagents (Invitrogen, USA). The transfection mixture contained siRNA (1 μg), Plus reagent (6 μl), and Lipofectamine (4 μl) in DMEM without serum (up to 100 μl). The transfection mixture was transferred to a 6-well plate, and fresh medium without serum was added (up to 1 ml). After a 3-h incubation, the medium containing the complexes was replaced with fresh medium (complete medium containing 10% fetal bovine serum) and incubated for an additional 12 h. Four replicates were performed for each experiment.

Transfection rate test. Coverglass culture was performed at the density of $5 \cdot 10^5$ cells/ml for 2-3 days. When two-thirds of the coverglass was covered with cells, fluorescently labeled siRNA (1 μg) was transfected and incubated as described above. After 12 h, cells were fixed with −4°C pre-cooled acetone and mounted with 70% glycerin without bubbles. Cells (n = 500) were counted under a Leica FW 4000 fluorescence microscope (Fluorescence Workstation, Germany). Transfection rate was calculated using the formula: (number of apoptotic cells/number counted) × 100%.

Screening for transfectants. *Real-time RT-PCR for mRNA assay.* Cells from each transfection group were collected, and real-time reverse transcription (RT)-PCR was performed using the One Step SYBER® RT-PCR kit (TaKaRa, China). Primers for real-time PCR were designed by Primer3 (http://frodo.wi.mit.edu/cgi-bin/primer3/primer3_www.cgi) according to the sequences of *M. musculus* SelW mRNA (Accession: BC052719) and *M. musculus* skeletal muscle actin mRNA (Accession: NM_009606) from GenBank. Primers for SelW: sense 5′CTA TAA GCC CAA GTA CCT CCA3′, anti-sense 5′CTG TAT CCA CAT AGC CAT CAC3′; primers for actin: sense 5′AGG ACC TGT ACG CCA ACA AC3′, anti-sense: 5′ACA TCT GCT GGA AGG TGG AC3′. The lengths of amplicons for target and housekeeping genes were 176 and 195 bp.

The RT-PCR pre-mixture was prepared by mixing 10 μl of 2× One Step SYBER RT-PCR buffer, 0.2 μl of MMLV reverse transcriptase (200 U/μl), 0.4 μl TaKaRa *Ex Taq* HS (5 U/μl), 0.4 μl of RNase inhibitor (40 U/μl), forward and reverse primers (0.4 μl each, $1 \cdot 10^{-5}$ M), and nuclease-free H_2O for a total volume of 18 μl. The reaction was started with the addition of 2 μl total RNA on a Rotor-Gene 3000 (Corbett Research, Australia). Total RNA extraction followed a modified Trizol protocol using 100% ethanol for RNA pellet washing. The RNA concentration was assayed by ultraviolet spectrophotometry (Beckman Du-640, Germany). The pre-mixture was maintained on ice and in the dark at all times prior to

real-time RT-PCR. The thermal profile for one-step SYBER RT-PCR reactions consisted of: 42°C for 15 min, 95°C for 2 min, and then 30-35 cycles of 95°C for 5 sec, 60°C for 30 sec. Optical graphs were obtained for each run, and melting curves were obtained immediately after completion of the PCR. Data were produced by plotting the fluorescence intensity against temperature as the temperature was increased from 55 to 95°C at 0.2°C/sec. Standard curves were constructed by performing real-time RT-PCR with 2-fold dilutions of standard RNA extracted from untreated cells and identified by routine sequencing. The C_t value obtained from the assay of each dilution was used to plot a standard curve. The standards curve for SelW was $y = -0.194x + 2.902$, and for the actin housekeeping gene was $y = -0.520x + 6.517$. R values of 0.99566 and 0.99705 (accepted range: $R = 0.9800 \sim 1$) for the standard curves of target and housekeeping genes, respectively, were obtained, and single predominant peaks of melting curves with high repeatability demonstrated the effectiveness of amplification. Quantitative assays of mRNA were normalized by the corresponding housekeeping genes.

Western blotting. Experiments were performed as described [4, 19] with rabbit polyclonal anti-SelW primary antibody and horseradish peroxidase–conjugated goat anti-rabbit IgG secondary antibody (Santa Cruz Biotechnology, USA). The result was collected by an ECL Detection kit (Amersham, USA) and assayed by Bandscan 5.0 software.

Detection of intracellular glutathione levels. The glutathione assay kit uses glutathione reductase to quantify intracellular levels of glutathione by measuring A_{405} according to the manufacturer's protocol (Beyotime Biotechnology, China) [20]. Absorbance measurements were obtained at 5-min intervals with five measurements per sample.

Cell viability assay. WST-1 (2-(4-iodophenyl)-3-(4-nitrophenyl)-5-(2,4-disulfophenyl)-2H-tetrazolium, monosodium salt) is an MTT (3-(4,5-dimethylthiazol-2-yl)-2,5-diphenyltetrazolium bromide)-like compound that can be reduced to yellowish-brown formazan by certain dehydrogenases. Lighter color implies a higher level of cellular cytotoxicity. As compared with MTT, WST-1 is more stable and sensitive, and thus yields more reliable results. At 12 h before transfection, cells from each transfection group were placed into a 96-well plate at 5000 cells/well. The transfection was performed as described above. At 12 h after transfection, the culture medium was replaced with fresh DMEM (100 µl) containing 10% fetal bovine serum and WST-1 solution (10 µl of the Beyotime Biotechnology solution). After incubation at 37°C for 1 h, the plate was transferred to a flatbed shaker for 1 min. The WST-1 assay was carried out at 450 nm on a microplate reader ELx 800 (Bio-Tek Instruments, USA), with 630 nm as the reference according to the manufacturer's instruction. Replicates of each condition were performed within one plate, and the protocol was replicated three to four times.

Apoptosis assay. *Fluorescent staining for detection of apoptosis.* Coverglass culture of cells and siRNA transfection were performed as described above. At 12 h after transfection, the medium in every well of a 6-well plate was replaced with fresh complete medium (DMEM + 10% fetal bovine serum), Hoechst 33342 (1 µl), and 1 µl propidium iodide (PI) (Fluorescent Staining Apoptosis Detection kit) (Vigorous Biotechnology Co., China), and the plate was incubated at 37°C in the dark for another 20 min. Following two washes with ice-cold phosphate-buffered saline (PBS), the cells were observed under a fluorescence microscope (Leica FW 4000). Apoptotic cells were identified based on the nuclear fragmentation and dense nuclear morphology and recorded in a continuous visual field (total number of cells >600). The percentage of apoptotic cells was calculated using the formula: (number of apoptotic cells/total number of counted cells) × 100%.

Flow cytometry for cell status. After transfection, cells were collected and resuspended in 1× binding buffer (10 mM Hepes/NaOH, pH 7.4, 140 mM NaCl, 2.5 mM $CaCl_2$) to adjust cell density to $1 \cdot 10^6$ cells/ml. This cell suspension (195 µl) was mixed with 5 µl annexin V/fluorescein isothiocyanate (FITC) (solution from Bender MedSystems, Austria) and incubated for 10 min at room temperature. Cells were then washed once with 1× binding buffer and resuspended in the same buffer (190 µl). Finally, the $3 \cdot 10^{-4}$ µM PI stock solution (10 µl) (Bender MedSystems) was added for flow cytometry analysis. Flow cytometry was performed with a Coulter Epics XL (Beckman Coulter) equipped with a 488-nm laser (15 mW). Fluorescence emission was monitored with a 525-nm filter for FITC, and a 620-nm filter for PI. The gate was set on FSC versus SSC parameters. Data for 5000 events were analyzed with SYSTEM II software routinely. The flow cytometry threshold was set to exclude cell debris.

Detection of intracellular antioxidative enzymes. *Detection of intracellular glutathione peroxidase (GPx).* The assay was performed using the Total Cellular Glutathione Peroxidase Assay kit (Beyotime Biotechnology). Cells were treated by 0.02% EDTA and then washed with and collected in PBS. Cells ($1 \cdot 10^6$) were then lysed with 200 µl of cell lysis buffer (20 mM Tris-HCl, pH 7.5, 150 mM NaCl, 1% (w/v) Triton X-100, 2.5 mM sodium pyrophosphate, 1 mM EDTA, 1% Na_3VO_4, 0.5 µg/ml leupeptin, 1 mM phenylmethanesulfonyl fluoride). The lysate was centrifuged at 12,000*g* at 4°C for 10 min, and the supernatant (20 µl) was then assayed. Reactions included sample (10 µl), glutathione peroxidase assay working solution (10 µl of 4.8 mM NADPH, 40.4 mM GSH, and glutathione reductase solution supplied by the manufacturer), cumene hydroperoxide (Cum-OOH, 4 µl of 15 mM), and glu-

tathione peroxidase assay buffer (up to 200 μl). Three blank (no sample) and three background (no Cum-OOH) controls were performed in the initial assay. The assay was performed at 25°C in an Ultrospec 1100 Pro ultraviolet spectrophotometer (Amersham Biosciences, USA) at 340 nm. One unit of glutathione peroxidase activity was defined as the amount required to oxidize 1 μmol NADPH to $NADP^+$ in 1 min at 25°C, pH 8.0.

Measurement of antioxidative enzymatic activity other than GPx. The levels of cellular superoxide dismutase (SOD), catalase (CAT), and total antioxidation capability (T-AOC) were measured using the respective assay kits from Nanjing Jiancheng (China). Briefly, $1 \cdot 10^6$ cells were collected after treatment with 0.1% trypsin and centrifuged at 1000*g* for 10 min. The cells were washed with PBS and homogenized with PBS (500 μl) on ice for 3 min. Lysates (50 μl) containing 40 μg of total protein were used to determine enzyme activity. The SOD assay was performed according to the manufacturer's instructions in an Ultrospec 1100 Pro ultraviolet spectrophotometer with a 1-cm light path at 550 nm. One unit of SOD activity was defined as the amount of SOD that produced one-half of the maximum competition against tris (2-benzimidazolylmethyl) amine in the specified system. The CAT assay was performed in the Ultrospec 1100 Pro with a 0.5-cm light path at 405 nm. One unit of CAT activity was defined as the amount of CAT required to decompose 1 μmol H_2O_2 per second. The T-AOC assay was performed in the Ultrospec 1100 Pro with a 1-cm light path at 520 nm. One unit of T-AOC activity was defined as an absorbance increase of 0.01 per minute. The enzyme activities were expressed as U/mg protein.

Statistical analysis. All experiments were repeated more than three times, and at least three samples were assessed for each assay according to the requirements of experimental design. One-way ANOVA and Tukey's HSD tests were performed using SPSS 10.0. Unless otherwise noted, probability values (P) less than 0.05 were considered statistically significant. The values are expressed as average ± S.D.

RESULTS

Screening of transfectants. *Transfection rate, mRNA, and protein in transfectants.* The transfection rate of cells transiently transfected with 21-bp synthetic fluorescently labeled siRNA was nearly 100%, as assessed by fluorescence microscopy (see color insert; Fig. 1, a and b). The SelW mRNA level was measured in each group, and the level in the siRNA-positive group decreased approximately 72.4% compared with the non-transfected group ($P < 0.05$), whereas the level in the negative control group decreased by an insignificant 0.93% (Fig. 2).

As determined by Western blotting, the SelW-specific siRNA significantly decreased the level of SelW protein

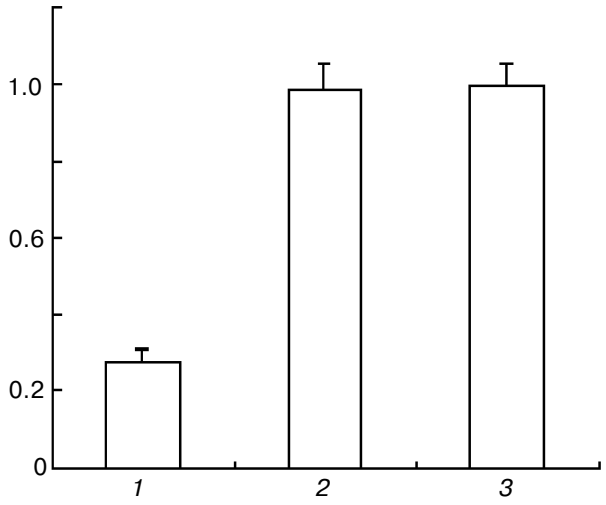

Fig. 2. SelW mRNA expression level among different experimental groups determined by real-time PCR. The relative values of SelW mRNA in SelW siRNA-transfected (*1*), negative (*2*), and blank control (*3*) groups were 0.275 ± 0.04, 0.9867 ± 0.01, and 0.996 ± 0.06, respectively. The *y* axis represents an amount of SelW mRNA in arbitrary units.

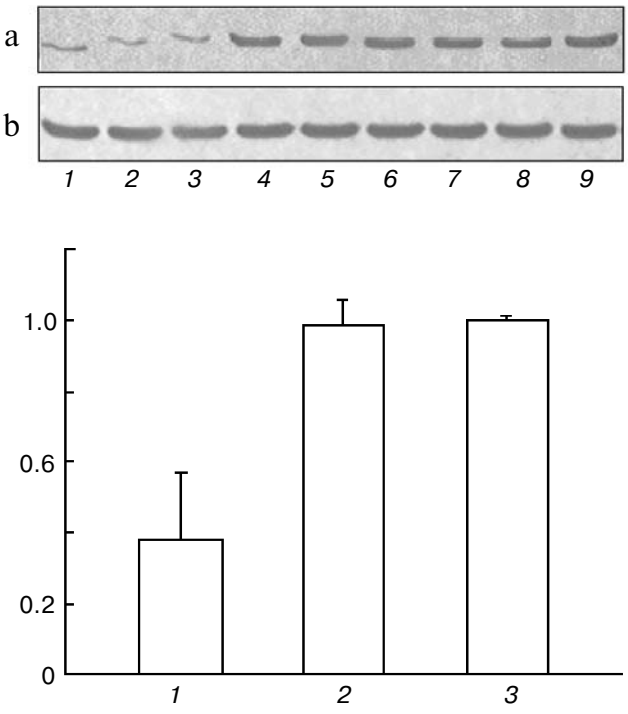

Fig. 3. Western blots analyzing SelW protein levels. a, b) Western blots of SelW and actin, respectively. Lanes: *1-3*) SelW siRNA-transfected group; *4-6*) negative control group; *7-9*) blank control. c) After normalizing the SelW level to the level of actin, the values of SelW in SelW siRNA-transfected (*1*), negative control (*2*), and blank control (*3*) groups were 0.378 ± 0.19, 0.988 ± 0.07, and 0.998 ± 0.014, respectively. The *y* axis represents the level of SelW expression in arbitrary units.

Activities and statistical analysis for WST-1, GSH, GPx, SOD, CAT, and T-AOC assays

Assay items	+siRNA positive group	+siRNA negative control group	–siRNA blank control group	$p1$	$p2$
WST-1	0.833 ± 0.05	1.102 ± 0.12	1.061 ± 0.07	$1.1 \cdot 10^{-5}$	0.44
GSH	0.218 ± 0.01	0.171 ± 0.004	0.168 ± 0.004	$6.04 \cdot 10^{-7}$	0.19
GPx*	4.87 ± 0.19	3.31 ± 0.11	3.30 ± 0.29	$5.55 \cdot 10^{-7}$	0.96
SOD**	80.77 ± 2.2	39.26 ± 0.23	39.78 ± 0.39	$5.85 \cdot 10^{-6}$	0.11
CAT**	6.43 ± 0.19	4.88 ± 0.08	4.91 ± 0.18	$1.10 \cdot 10^{-6}$	0.72
T-AOC**	2.341 ± 0.26	0.797 ± 0.19	0.766 ± 0.21	$4.8 \cdot 10^{-7}$	0.80

Note: Values are expressed as the mean ± S.D. $p1$, statistical differences between the SelW siRNA-transfected group and blank control group; $p2$, statistical differences between negative and blank control groups. $P < 0.05$ was considered significant.

* mU/ml, where U is μmol/min or μmol/sec.

** U/mg protein.

by 62.1% ($P < 0.01$), whereas there was no significant change in the level in the negative control group compared with the non-transfected control (Fig. 3).

Measurement of glutathione level in SelW-specific siRNA transfectant. Based on the glutathione assay, there was a significant increase (30.0%; $P < 0.05$) in glutathione production in SelW siRNA-transfected cells as compared with the non-transfected control. However, there was no significant difference in glutathione production between the negative control and blank control groups (the table).

Cell viability. In the WST-1 assay, the viability of the SelW siRNA-transfected group decreased significantly by 21.5% compared with the blank control ($P < 0.05$). However, there was no significant difference in cell viability between the negative and blank control groups (the table).

Induction of apoptosis. We assessed apoptosis by fluorescence staining. Fluorescently labeled cells having dense bright blue fluorescence, a meniscus shape, and segmented were considered apoptotic. Based on these criteria, 34.6% of SelW siRNA-transfected cells were apoptotic (see color insert: Fig. 1, c and d).

Using the flow cytometry assay, the proportions of apoptotic (PI–/FITC+), normal (PI–/FITC–), and necrotic (PI+/FITC+) cells from each group were reported by the SYSTEM II software. The proportion of apoptotic cells in the SelW siRNA-transfected, negative control, and blank control groups was 37.5, 0.94, and 0.7%, respectively (Fig. 4).

Measurement of antioxidative enzymes. The activity of certain antioxidative enzymes in SelW siRNA-transfected cells increased significantly ($P < 0.05$) compared with the non-transfected control group: GPx (+47.6%), SOD (+103.0%), CAT (+31.0%), and T-AOC (+205.6%). There were no significant differences in the activities of these enzymes between the negative and blank control groups (the table).

DISCUSSION

In this study, SelW expression and mRNA levels were significantly downregulated by RNA interference using a double-stranded SelW-specific siRNA in transient transfections. As expected, depletion of SelW was cytotoxic. In the apoptosis assay, both flow cytometry and fluorescence staining indicated increased levels of apoptosis. As a consequence of SelW depletion, the activities of SOD, CAT, GPx, and T-AOC and the amount of glutathione increased significantly as compared to the negative and blank controls.

Redox regulation has emerged as an essential regulatory process of many pathways in cell biology [21, 22]. Disruption of the intracellular redox balance leads to a state of oxidative stress, during which proteins, nucleic acids, lipids, and other macromolecules can undergo severe damage [23, 24]. Reactive oxygen species of chemical or metabolic origin can cause oxidative stress in cells, resulting in oxygen cytotoxicity; such reactive oxygen species, however, can be scavenged in enzyme-catalyzed or non-enzyme-catalyzed reactions. Reactive oxygen species can alter the activities of cellular proteins and deplete free radical scavengers. Thus, antioxidant enzymes respond to oxidative stress by inducing gene expression and by changing their activity and subcellular localization [25-27]. Conformational changes in enzymes can result in their activation, deactivation, or changes in their activities [28, 29]. Antioxidative enzymes such as SOD, CAT, and GPx are responsible for clearing superoxide anion radicals, hydrogen peroxide, and lipid peroxides in cells [30]. In our present study, the increased activities of SOD, CAT, and GPx as well as the increased levels of glutathione upon downregulation of SelW illustrated that the homeostasis of antioxidative systems in muscle cells was perturbed. Indeed, we did not observe decreases in the antioxidative capability of muscle cells

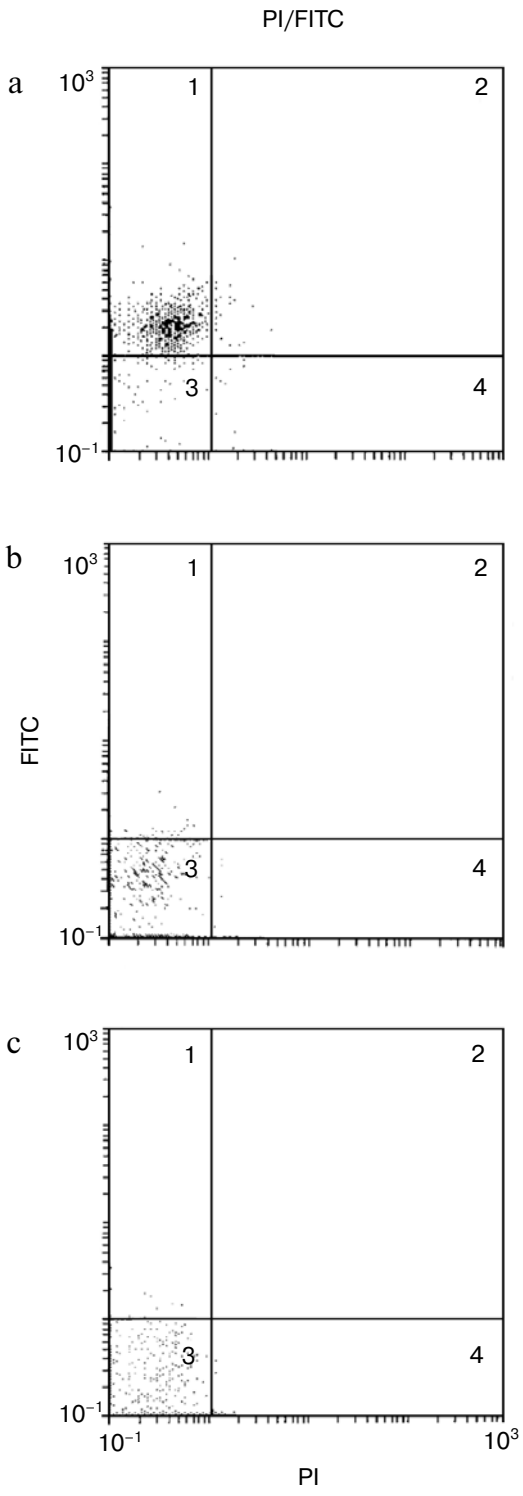

Fig. 4. Flow cytometry analysis of apoptosis for each transfection group: a) SelW siRNA-transfected group: apoptosis rate 37.5%, normal rate 59.7%, death rate 2.04%; b) negative control group: apoptosis rate 0.94%, normal rate, 98.9% death rate 0.02%; c) blank group: apoptosis rate 0.7%, normal rate 97.9%, death rate 0.00%. Quadrants 1, 2, 3, and 4 represent apoptotic cells (FITC+/PI–), cells in late apoptosis (FITC+/PI+), normal cells (FITC–/PI–), and damaged cells (FITC–/PI+).

upon SelW depletion, implying a compensatory response by the above mentioned enzymes and perhaps other unknown enzymes as well.

Decreases in cellular antioxidative capabilities are one of the primary forces that drive apoptosis. In our study, however, SelW-depleted cells did not undergo apoptosis because of oxidative stress. The relationship between apoptosis and SelW depletion in our study suggests that SelW plays an important role in apoptosis regulation. A study by Lescure et al. [31] suggested that regulation of intracellular calcium concentrations might be a general function of selenoproteins. SelW potentially regulates the activities of 14-3-3 proteins, which play a role in signal transduction in the heart [16]. By combining the clinical pathological characteristics of calcification of skeletal and cardiac muscles associated with a reduction in SelW, we hypothesize that the regulation of calcium levels might be the main function of SelW. Currently there is no method corresponding to RNA interference with regard to effectiveness and stability that would increase the expression of target proteins, and thus we were unable to overexpress SelW as a control. It is difficult to perform oxidative stress via oxidizing reagents to analyze the antioxidative capabilities of target proteins and muscle cells by transient transfection. As such, implementation of a calcium regulation assay in SelW-depleted cells would be helpful to better understand the function of SelW.

This study was supported by the China Postdoctoral Science Foundation (LRB06-262) and Heilongjiang Postdoctoral Financial Assistance (LBH-Z07250).

REFERENCES

1. Pappas, A. C., Zoidis, E., Surai, P. F., and Zervas, G. (2008) *Comp. Biochem. Physiol. B. Biochem. Mol. Biol.*, **151**, 361-372.
2. Vendeland, S. C., Beilstein, M. A., Chen, C. L., Jensen, O. N., Barofsky, E., and Whanger, P. D. (1993) *J. Biol. Chem.*, **268**, 17103-17107.
3. Ream, L. W., Vorachek, W. R., and Whanger, P. D. (2003) in *Selenium: Its Molecular Biology and Role in Human Health* (Hatfield, D. L., ed.) Kluwer Academic Publishers, London, pp. 141-145.
4. Yeh, J. Y., Beilstein, M. A., Andrews, J. S., and Whanger, P. D. (1995) *FASEB J.*, **9**, 392-396.
5. Whanger, P. D. (2000) *Cell Mol. Life Sci.*, **57**, 1846-1852.
6. Gu, Q. P., Sun, Y., Ream, L. W., and Whanger, P. D. (2000) *Mol. Cell Biochem.*, **204**, 49-56.
7. Pagmantidis, V., Bermano, G., Villette, S., Broom, I., Arthur, J., and Hesketh, J. (2005) *FEBS Lett.*, **579**, 792-796.
8. Papp, L. V., Lu, J., Holmgren, A., and Khanna, K. K. (2007) *Antioxid. Redox. Signal.*, **9**, 775-806.
9. Lu, J., and Holmgren, A. (2009) *J. Biol. Chem.*, **284**, 723-727.
10. Beilstein, M. A., Vendeland, S. C., Barofsky, E., Jensen, O. N., and Whanger, P. D. (1996) *J. Inorg. Biochem.*, **61**, 117-124.

11. Gu, Q. P., Beilstein, M. A., Vendeland, S. C., Lugade, A., Ream, W., and Whanger, P. D. (1997) *Gene*, **193**, 187-196.
12. Whanger, P. D., Vendeland, S. C., Gu, Q. P., Beilstein, M. A., and Ream, L. W. (1997) *Biomed. Environ. Sci.*, **10**, 190-197.
13. Jeong, D., Kim, T. S., Chung, Y. W., Lee, B. J., and Kim, I. Y. (2002) *FEBS Lett.*, **517**, 225-228.
14. Bauman, A. T., Malencik, D. A., Barofsky, D. F., Barofsky, E., Anderson, S. R., and Whanger, P. D. (2004) *Biochem. Biophys. Res. Commun.*, **313**, 308-313.
15. Loflin, J., Lopez, N., Whanger, P. D., and Kioussi, C. (2006) *J. Inorg. Biochem.*, **100**, 1679-1684.
16. Aachmann, F. L., Fomenko, D. E., Soragni, A., Gladyshev, V. N., and Dikiy, A. (2007) *J. Biol. Chem.*, **282**, 37036-37044.
17. Dikiy, A., Novoselov, S. V., Fomenko, D. E., Sengupta, A., Carlson, B. A., Cerny, R. L., Ginalski, K., Grishin, N. V., Hatfield, D. L., and Gladyshev, V. N. (2007) *Biochemistry*, **46**, 6871-6882.
18. Sun, Y., Gu, Q. P., and Whanger, P. D. (2001) *J. Inorg. Biochem.*, **84**, 151-156.
19. Yeh, J. Y., Ou, B. R., Forsberg, N. E., and Whanger, P. D. (1997) *BioMetals*, **10**, 11-22.
20. Jia, J. H., Wang, Y., Cao, Y. B., Gao, P. H., Jia, X. M., Ma, Z. P., Xu, Y. G., Dai, B. D., and Jiang, Y. Y. (2007) *Biochem. Biophys. Res. Commun.*, **359**, 163-167.
21. Linke, K., and Jakob, U. (2003) *Antioxid. Redox. Signal.*, **5**, 425-434.
22. Ghezzi, P. (2005) *Free Radic. Res.*, **39**, 573-580.
23. Barzilai, A., Rotman, G., and Shiloh, Y. (2002) *DNA Repair (Amst).*, **1**, 3-25.
24. Gille, G., and Sigler, K. (1995) *Folia Microbiol.*, **40**, 131-152.
25. Hirota, K., Matsui, M., Iwata, S., Nishiyama, A., Mori, K., and Yodoi, J. (1997) *Proc. Natl. Acad. Sci. USA*, **94**, 3633-3638.
26. Karimpour, S., Lou, J., Lin, L. L., Rene, L. M., Ma, X., and Karra, S. (2002) *Oncogene*, **21**, 6317-6327.
27. Hattori, H., Imai, H., Furuhama, K., Sato, O., and Nakagawa, Y. (2005) *Biochem. Biophys. Res. Commun.*, **337**, 464-473.
28. Nordberg, J., and Arner, E. S. J. (2001) *Free Radic. Biol. Med.*, **31**, 1287-1312.
29. Xia, L., Nordman, T., Olsson, J. M., Damdimopoulos, A., Bjorkhem-Bergman, L., Nalvarte, I., Eriksson, L. C., Arner, E. S. J., Spyrou, G., and Bjorstedt, M. (2003) *J. Biol. Chem.*, **278**, 2141-2146.
30. Yusof, Y. A. M., Ahmad, N., Das, S., Sulaiman, S., and Murad, N. A. (2009) *African J. Tradition., Compliment. Altern. Med.*, **6**, 87-93.
31. Lescure, A., Rederstorff, M., Krol, A., Guicheney, P., and Allamand, V. (2009) *Biochim. Biophys. Acta*, **1790**, 1569-1574.